Published in Materials Research Bulletin, 2005

Processing Microstructure Property Correlation of Porous Ni-YSZ Cermets Anode for SOFC Application

Swadesh K Pratihar[1], A. Dassharma[*] and H.S. Maiti[*]
Department of Ceramic Engineering
National Institute of Technology
Rourkela – 769 008 India

Abstract

The present paper investigates microstructural properties and electrical conductivity of cermets prepared by a solid-state technique, a liquid-dispersion technique and a novel electroless coating technique. The Ni-YSZ processed through different techniques shows varying temperature-conductivity behaviour. The cermets synthesized by electroless coating were found to be electronically conducting with 20 volume % Nickel, which is substantially lower than that normally reported. The conductivity of Ni-YSZ cermets was found highest for the samples prepared by an electroless coating technique and lowest for the samples prepared by a solid-state technique, the samples prepared from liquid-dispersion show an intermediate value for a constant nickel content. The variation in electrical conductivity has been well explained from the microstructure of the samples.

Keywords: Solid oxide fuel cell; Cermet anode; Processing; Microstructure

1. Corresponding author: Tel: 91 661 2462206; Fax: 91 661 247 2926
E-mail: skpratihar@nitrkl.ac.in (S.K. Pratihar)

* Electroceramics Division, Central Glass & Ceramic Research Institute, Kolkata – 700 032, India.

1. Introduction

Solid oxide fuel cells (SOFC) are important as energy conversion systems due to their high efficiency, design modularity and environmentally friendly nature. The most popular anode material for solid oxide fuel cells (SOFC) is a nickel yttria stabilized zirconia (Ni-YSZ) cermet [1-3]. In order to achieve the best performance of an anode cermet, it should satisfy the following criteria: a) high electrical conductivity to reduce the ohmic loss, b) enough electrochemical activity to reduce the activation polarization and c) proper microstructural conditions to reduce the concentration polarization, which is related to the diffusion of the reactant or product of the electrode reaction. These factors are necessary to obtain the best performance of the anode and

partial fulfillment of those conditions is not sufficient for the proper operation of a SOFC. For example, for higher electrical conductivity, higher Ni content is the best choice**,** but; higher Ni content leads to instability of microstructure due to large Ni coarsening and thermal expansion coefficient mismatch. On the other hand, for lower concentration polarization, a highly porous composite is better, but cannot guarantee the proper mechanical and electrical properties. Open porosity is required for the anode to supply fuel and for removal of reaction products. The nickel particles forming a percolative network have a large catalytic activity and are responsible for transporting electrons from the electrode reaction site to the current collector. The addition of YSZ is necessary to support the nickel particles, to inhibit coarsening by sintering into larger particles at the usual operating temperature of an SOFC, and to give the cermet a thermal expansion coefficient close to that of other cell components [4-7]. Literature on Ni-YSZ cermet synthesis [8-10] describes uniform and homogeneous distribution between the Ni and YSZ phases in the matrix. However, cermets prepared by these techniques behave as biphasic composites and shows percolation conductivity at 35-40 volume % Ni depending on the process parameter. Although such a high amount of Ni meets the conductivity requirement of SOFC anodes along with the porosity requirement (35-40 %) for lowering concentration polarization, it has a higher thermal expansion coefficient than the other cell components. The electrical property of Ni-YSZ cermet as an anode is greatly influenced not only by the electrical conductivity of the each constituent component, but also by microstructural parameters like distribution and contiguity of each phase component. The later is strongly dependent on powder preparation techniques and fabrication processes.

In this investigation, the Ni-YSZ cermet material was prepared by three different routes in order to study the effect of powder preparation technique on microstructure and electrical conductivity of the samples. Ni-YSZ samples containing 5-60 volume % Ni has been prepared by three different routes namely solid-state, liquid-dispersion and electroless coating. Solid-state technique is a conventional route, widely used for synthesis of Ni-YSZ cermets. Attempts have been made to have a uniform distribution of Ni and YSZ in the sample matrix for the powder synthesized by liquid-dispersion techniques. We have reported the detailed powder synthesis technique earlier [11]. The metallic conductivity of the Ni-YSZ cermet is the results of the formation of a Ni-to-Ni percolative network in the samples. In view of this a metallic coating of

Ni was applied on YSZ particles using an electroless coating technique. The detailed coating process has been reported earlier [12]. Attempts have been made to correlate the electrical conductivity of the samples as a function of microstructure and the powder synthesis technique.

2. Experimental

The Ni-YSZ cermets (nickel content 5-60 volume % of total solids) studied in this present investigation were prepared by a) conventional solid-state technique, b) liquid-dispersion technique and c) electroless coating technique. The starting YSZ powder was 8 mole% yttria stabilized zirconia powder (TZ-8Y, Tosoh Corporation, Japan). In the solid-state technique YSZ powder was mixed with NiO powder (E-mark, India) in an agate mortar using acetone as medium for about 4 h. The mixture was then dried in an oven at 100^{o}C. In the liquid-dispersion technique, TZ-8Y powders were dispersed in a nonaqueous solution of nickel nitrate, which was then evaporated to dryness on a magnetic stirrer-cum-hot plate. During the drying process the YSZ powder was kept suspended by vigorous magnetic stirring. This dried mass was then calcined at 800^{o}C for 2 h to yield NiO-YSZ powder. The detail description of this process is reported elsewhere [11]. In the electroless coating technique TZ-8Y powder was coated with metallic nickel using electroless coating. Prior to electroless Ni coating the YSZ powders were sensitized and catalyzed using $SnCl_2$ and $PdCl_2$ solutions. These catalyzed powders were then coated with Ni by treating with an electroless nickel bath. Throughout the coating process the powders were kept suspended by vigorous stirring. The detailed deposition study was reported earlier [12]. The Ni content in the electroless coated samples was estimated using thermogravimetry (TGA). The synthesis was performed with small batches and repeated several times, which gives a constant result. The powder prepared by these techniques was then pressed in the shape of a rectangular bar 15mm x 3mm x 2mm following conventional pressing. These pressed pellets were sintered in the temperature range 1200^{o}C-1350^{o}C for 2-6 h in air. During this sintering process the nickel coated YSZ samples also converts to a NiO-YSZ composite. The air sintered samples were then reduced under hydrogen + argon (H_2 + Ar) atmosphere in a tube furnace at 900^{o}C/2 h in order to reduce NiO to metallic Ni. Constant sample porosity in hydrogen reduced samples (35 % required for actual operation) has been attained in the samples by tailoring the sintering conditions. Electrical conductivity of the cermet was measured in the temperature range from ambient to 1000^{o}C under reducing (H_2 + Ar) atmosphere by a four probe

DC technique using a 7 digit HP 3458A multimeter. Unfluxed platinum paste was used as a contact for electrical measurements. Microstructural evaluation was also performed using scanning electron microscopy (LEICA S440). Ni and Zr elemental distribution have been performed by global EDX mapping.

3. Results and Discussion

The microstructural features present in Ni-YSZ composites are Ni and YSZ phases and porosity. The size, shape and distribution of these phases are important for the different properties of the anode. The anode microstructure has been found to be strongly dependent on the processing techniques. In order to find out the distribution of Ni and YSZ phases within the samples back scattered SEM was utilized. The following section discuses the different microstructural features of the samples in the light of processing techniques.

The microstructure (SEM back scattered image, Zr and Ni distribution) of Ni-YSZ cermet containing 40 volume % Ni prepared by solid-state technique is presented in Fig. 1. A porous structure can be observed from this back scattered image (Fig. 1 a), while, the Zr and Ni distribution in the cermet matrix is presented in Fig. 1 (b & c) respectively. A very inhomogeneous distribution of zirconia and nickel within the composite matrix can be observed in this microstructure. This inhomogeneous distribution of the two phases may come from the very nature of the processing technique used for preparation of the composite powder.

Figure 2 represents a representative back scattered image along with Zr and Ni distribution for the sample containing 40 volume % nickel prepared by liquid-dispersion technique. A porous microstructure are observed in back scattered image (Fig. 2 a). A fairly uniform distribution of Zr (Fig. 2 b) and that of Ni (Fig. 2 c) are also observed. Thus the microstructure contains very fine and homogeneous distribution of Ni and YSZ particles due to improved processing of the liquid-dispersion technique compared to that produced from the solid-state technique Fig. 1.

A typical back scattered image of 40 volume % Ni-YSZ composite along with Zr and Ni mapping is shown in Fig. 3 for the samples prepared using an electroless coating technique. Formation of a continuous nickel ring around the YSZ particles can be visualized easily from

Fig. 3 (c). This also indicated the effectiveness of the electroless coating technique. Though Fig. 3 (b) indicates some large zirconia particles; under higher magnification it is seen that these zirconia particles are actually a cluster of nickel coated, fine YSZ powder. The interlinking of nickel particles around YSZ particle clusters can be seen in Fig. 3 (c). A combination of the Fig. 3 (b) and (c) together will result in Fig. 3 (a). The porous structure can also be seen in Fig. 3 (a). The microstructure is quite different from that observed for the solid-state (Fig. 1) and liquid-dispersion technique (Fig. 2). This was possible due to the nature of the preparation technique adopted in this case.

The composite samples undergo some change in porosity when the air sintered samples are reduced under H_2 + Ar atmosphere at high temperatures. SEM fractographs of the samples are studied in order to study this porosity change. SEM fractographs of an air sintered and reduced samples containing 40 volume % nickel prepared by a liquid-dispersion technique are presented in Fig. 4. An increase in overall porosity is observed in a reduced specimen (Fig. 4 b) in comparison to that of an air sintered specimen (Fig. 4 a). The increase in porosity results from the conversion of NiO to metallic nickel during reduction. Radovic et al. [13] also reported the increase in porosity of Ni-YSZ cermet on hydrogen reduction. They suggested that the porosity of NiO-YSZ composite before and after hydrogen reduction bears a linear relationship as a function of the nickel content. Although the porous structure of the composite is evident from the SEM factrograph (Fig. 4) YSZ and metallic nickel particles could not be clearly resolved.

Figure 5 represents the SEM fractographs of 40 volume % Ni-YSZ sample prepared using the electroless Ni coated YSZ powder before and after reduction. Fig. 5 (a) represents the sample before reduction and (b) represents it after reduction. It is clear from the micrograph that an increase in porosity of the samples occurs upon reduction. This is due to the fact that upon reduction, NiO in the air sintered samples is converted to metallic Ni. This conversion may be attributed to an increase in porosity due to loss of oxygen as well as the crystallographic change. However, the two different phases namely NiO or Ni and YSZ are not clearly resolved from the microstructure. The most interesting feature is that the samples prepared by a liquid-dispersion technique show a larger grain size compared to the samples prepared using the electroless coating technique. This may be due to the inhibition of sintering fine YSZ powder. This was made possible by coating the YSZ powder by metallic Ni.

The electrical conductivity of 40 volume % Ni-YSZ cermet (which is always above the percolation threshold) containing 35 % porosity and prepared by all the above three techniques is given in Fig. 6. Samples of 35 % porosity have been prepared by tailoring the sintering conditions. It is interesting to note that the conductivity of the samples prepared by the solid-state technique has the lowest conductivity, whereas specimens prepared by the electroless coating technique have the highest value. The conductivity of the samples prepared by the liquid-dispersion technique is intermediate (between these two). This trend has been observed in all the samples containing 30 – 60 volume % nickel prepared by these three methods. The results could be explained from the consideration of the extent of homogeneity in the distribution of the two phases present in the samples. In the solid-state technique, the inherent processing inhomogenity in the samples results in poor conductivity over the entire composition range. The microstructure of the Ni-YSZ sample prepared by this technique also shows a non-uniform distribution of Ni and YSZ phases (Fig. 1). The samples prepared by the liquid-dispersion technique, on the other hand show higher conductivity compared to the solid-state technique due to uniform and intimate distribution of the two phases resulting from better mixing. Microstructure of the cermet prepared by this technique also shows a very homogeneous distribution of Ni and YSZ phases in its matrix (Fig. 2). The samples prepared by the electroless coating technique, however, show the highest conductivity due to uniform coating of the YSZ particles by metallic nickel, which provides the best possible connectivity of the Ni phase and therefore, the metallic conduction path, as depicted by microstructural observation (Fig. 3).

The electrical conductivity of the samples as a function of nickel concentration measured at 1000^{o}C is plotted in Fig. 7 for the three different powder preparation techniques. The variation of conductivity with Ni content shows S-shaped curves for each of the three preparation techniques. The conductivity of samples measured at 1000^{o}C containing 10 – 60 volume % nickel and prepared by solid-state technique have the lowest value, while that prepared by the electroless coating technique have the highest value. Once again the conductivity of the cermets prepared by the liquid-dispersion technique has an intermediate value. For both the solid-state and liquid-dispersion techniques the samples exhibit a sudden jump in conductivity corresponding to the electrical continuity/discontinuity transition point of the dispersed nickel phase at around 30 volume % nickel. The sample prepared by solid-state and liquid-dispersion

techniques behave as a biphasic system consisting of Ni and YSZ. Hence, this electrical continuity/discontinuity transition at around 30 volume % Ni can be explained from percolation/effective media theory. The percolation threshold is revealed to be influenced by many variables such as the porosity, pore size, size distribution, and size of raw powders as well as contiguity of each constituent component. The electrical behavior of Ni/YSZ cermets is, therefore, a strong function of these factors [14,15].

On the other hand, the cermets prepared by electroless coating show a similar transition as low as 20 volume % nickel. The samples prepared by this technique will not behave as a biphasic system due to very nature of the preparation technique used here. In this case, the conductivity transition results from a uniform nickel coating on the YSZ particle, which provides a more intimate nickel-to-nickel contact, at a much lower overall metal content.

However, the high electronic conductivity provided by an interconnecting network of Ni particles do not necessarily provide a good performance of the anode in SOFC. The charge transfer reaction occurs at the triple points - YSZ particle, Ni particle and gas phase. Oxygen ions diffuse through YSZ particles and react in the triple points with hydrogen ions. Thus, it is important to have an interconnected network of YSZ particles, too. This interconnected YSZ network extends the triple phase boundary, which in turn reduces the polarization loss at the anode [16]. In cathode supported SOFCs, the anode layer will be very thin (150-200 μm), thus for this particular SOFC design the triple points will be limited on the YSZ electrolyte surface only. Hence, this material may be suitable for cathode supported SOFCs designs.

4. Conclusion

Electrical conductivity of Ni-YSZ cermets is strongly dependent on the powder synthesis technique as well as the microstructure.

Uniform and homogeneous distribution of Ni and YSZ provides better electrical conductivity for the samples prepared by the liquid-dispersion technique.

The conductivity percolation thresholds for cermets prepared by solid-state and liquid-dispersion technique is around 30 volume % Ni and follows biphasic percolation theory.

The continuity/discontinuity transition is around 10-20 volume % Ni for samples prepared by the electroless coating technique is possible due to a uniform and homogeneous Ni coating on the YSZ particles.

References

[1] N.Q. Minh, J. Am. Ceram. Soc. 76 (1993) 563.
[2] S.P.S. Badwal and K. Foger, Ceramic International 22 (1996) 257.
[3] N.Q. Minh and T. Takahashi, Science and Technology of Ceramic Fuel Cells, Elsevier, New York, 1995.
[4] D.E. Dees, T.D. Claar, T.E. Easler, D.C. Fee and F.C. Mrazek, J. Electrochemical Soc. 134 (1987) 2141.
[5] J. Mizusaki, S. Tsuchiya, K. Waragai, H. Tagawa, A. Yoshihidi and Y. Kuwayama, J. Am. Ceram. Soc. 79 (1996) 109.
[6] G. Maggio, I. Ielo, V. Antonucci and N. Giordano, in : F. Grosz, P. Zegers, S.C. Singhal and O. Yamamoto (Eds.), Solid Oxide Fuel Cells II, The Commission of the European Communities, Luxembourg, 1991, pp. 611- 620.
[7] G.E. Pike and C.H. Seager, J. Appl. Phys. 48 (1997) 5152.
[8] M. Marinsek, K. Zupan and J. Macek, J. Power Sources 86 (2000) 383.
[9] Y. Li, Y. Xie, J. Gong, Y. Chen and Z. Zhang, Mat. Sci. Engg. B 8 (2001) 119.
[10] S.T. Aruna, M. Muthuraman and K.C. Patil, Solid-state Ionics 111 (1998) 45.
[11] S.K. Pratihar, R.N. Basu, S. Mazumdar, H.S. Maiti, Solid Oxide Fuel Cells (SOFC VI), Proceedings vol. 99-19, Electrochemical Society,1999, p. 513.
[12] Swadesh K. Pratihar, A. Das Sharma, R.N. Basu and H.S. Maiti, Journal of Power Sources 129 (2004)138.
[13] M. Radovic and E. Lara-Curzio, Acta. Mat. 52 (2004) 5747.
[14] H. Itoh, T. Yamamoto, M. Mori, T. Horita, N. Sakai, H. Yokokawa, M. Dokiya, J. Electrochem. Soc. 144 (1997) 641.
[15] T. Iwata, J. Electrochem. Soc. 143 (1996) 1521.
[16] M. Mori, T. Yamamoto, H. Itoh, H. Inaba, H. Tagawa, in: U. Stimming, S.C. Singhal, H. Tagawa, W. Lehnert (Eds.), in Proceedings of the Fifth International Symposium on Solid Oxide Fuel Cells (SOFC-V), Aachen, Germany, 2–5 June 1997, p. 869.

List of Figures

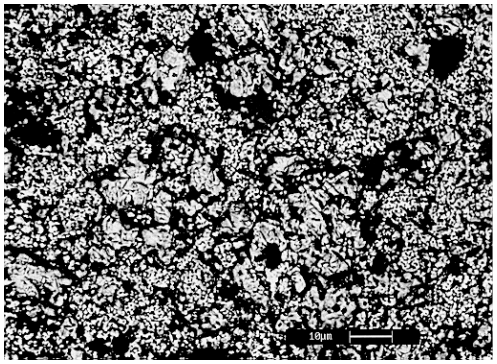

(a)

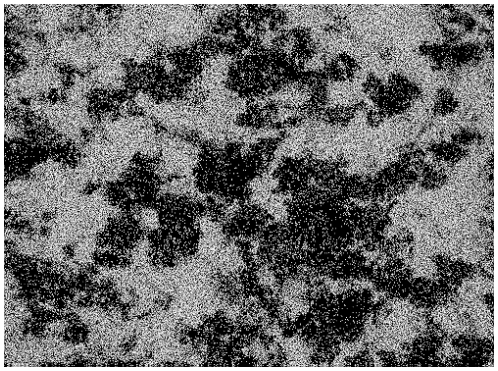

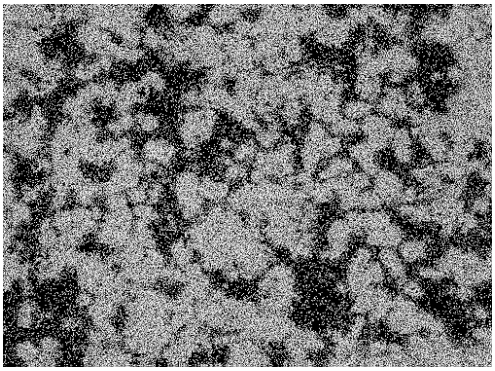

(b) (c)

Fig.1

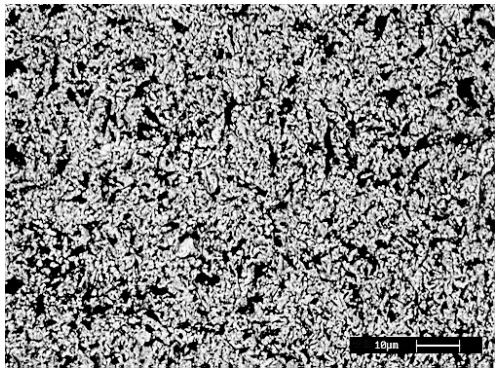

(a)

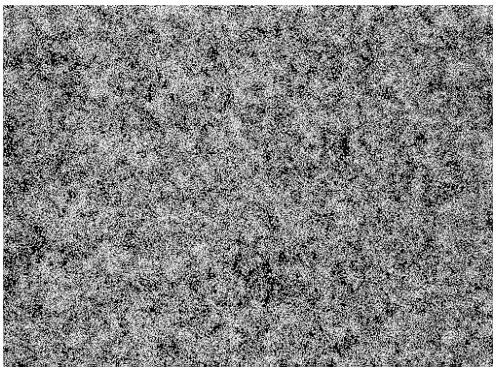

(b)

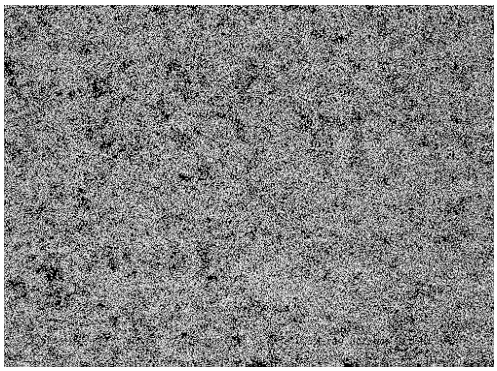

(c)

Fig.2

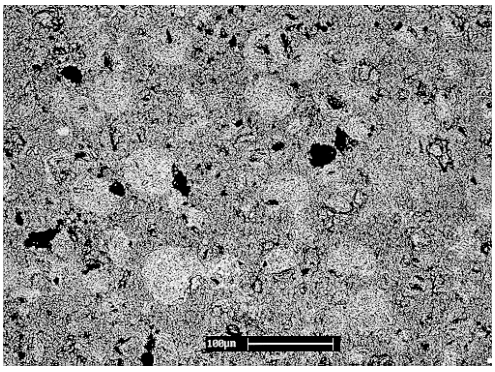

(a)

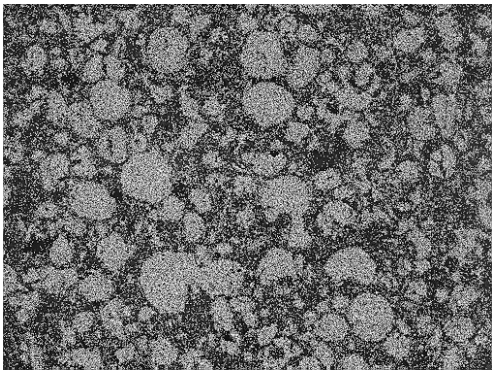

(b)

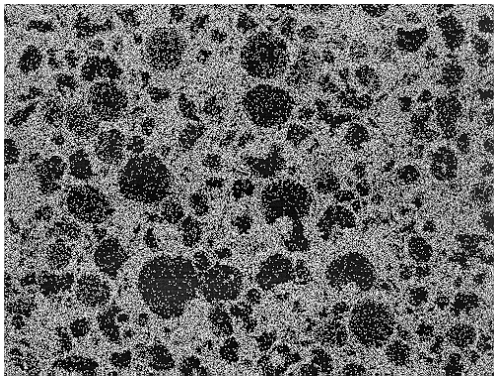

(c)

Fig.3

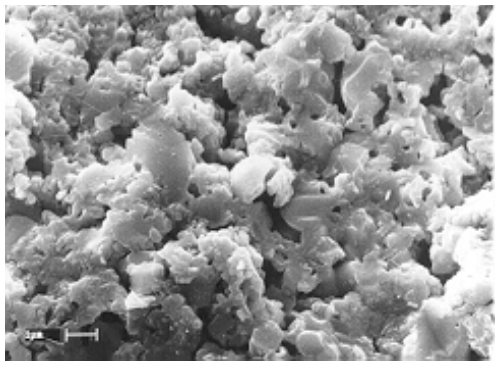

(a)

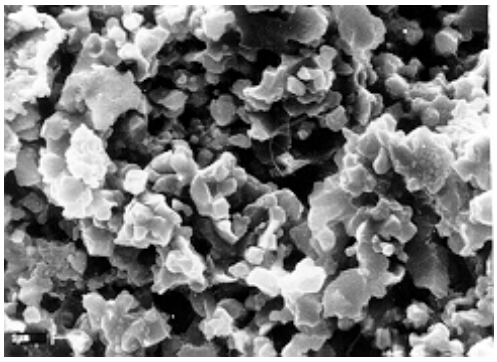

(b)

Fig.4

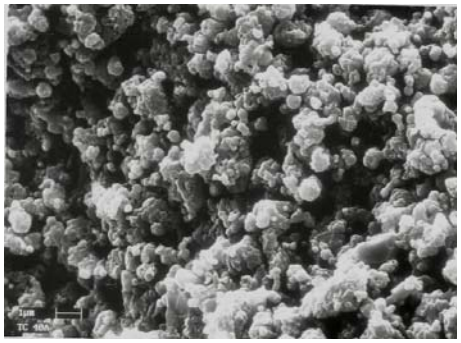

(a)

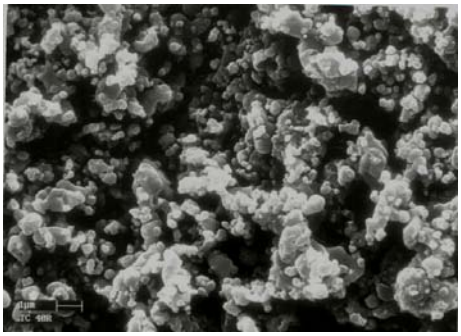

(b)

Fig.5

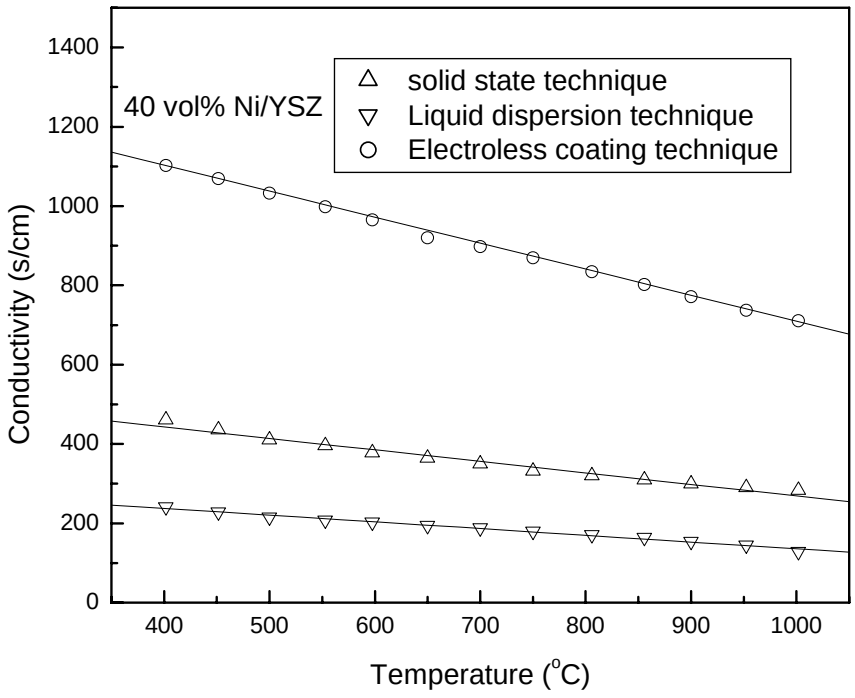
40 vol% Ni/YSZ
solid state technique
Liquid dispersion technique
Electroless coating technique
Conductivity (s/cm)
Temperature (°C)
0
200
400
600
800
1000
1200
1400
400
500
600
700
800
900
1000

Fig.6

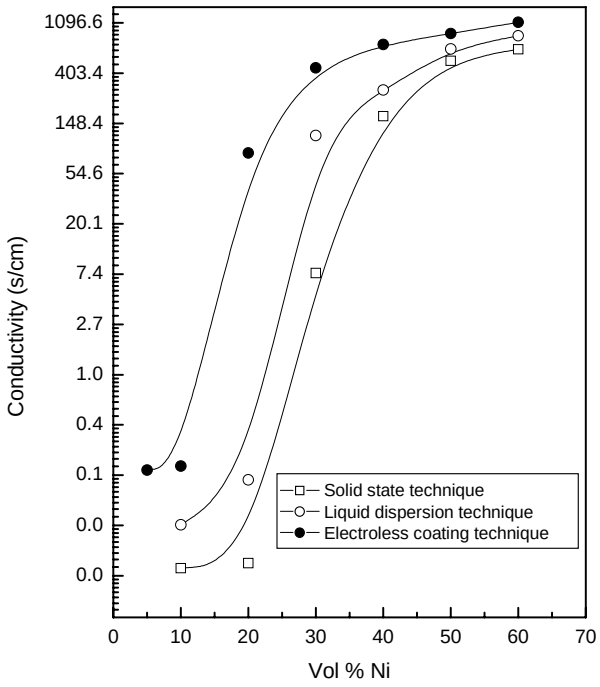
1096.6
403.4
148.4
54.6
20.1
7.4
2.7
1.0
0.4
0.1
0.0
0.0
Conductivity (s/cm)
0
10
20
30
40
50
60
70
Vol % Ni
Solid state technique
Liquid dispersion technique
Electroless coating technique

Fig.7